

1 *Type of the Paper (Article)*

2 **Improvement of performance, stability, and** 3 **continuity by modified size-consistent** 4 **multipartitioning QM/MM method**

5 **Hiroshi C. Watanabe**^{1,2,3*}

6 ¹ Faculty of Science and Technology, Keio University, 3-14-1 Hiyoshi, Kohoku-ku, Kawasaki, 223-8522,
7 Japan

8 ² Keio Quantum Computing Center, Keio University, 3-14-1 Hiyoshi, Kohoku-ku, Kawasaki, 223-8522, Japan

9 ³ Japan Science and Technology Agency, PRESTO 4-1-8, Honcho, Kawaguchi, Saitama, 332-0012, Japan,

10

11 * Correspondence: hcwatanabe@keio.jp; Tel.: +81-45-566-1817

12

13 **Abstract:** For condensed systems, the incorporation of quantum chemical solvent effects into
14 molecular dynamics simulations has been a major concern. To this end, quantum
15 mechanical/molecular mechanical (QM/MM) techniques are popular and powerful options to treat
16 gigantic systems. However, they cannot be directly applied because of temporal and spatial
17 discontinuity problems. To overcome these problems, in a previous study, we proposed a corrective
18 QM/MM method, size-consistent multipartitioning (SCMP) QM/MM, and successfully
19 demonstrated that, using SCMP, it is possible to perform stable molecular dynamics simulations by
20 effectively taking into account solvent quantum chemical effects. The SCMP method is characterized
21 by two original features: size-consistency of a QM region among all QM/MM partitioning and
22 partitioning update. However, in our previous study, the performance was not fully elicited
23 compared to the theoretical upper bound, and the optimal partitioning update protocol and
24 parameters were not fully verified. To elicit the potential performance, in the present study, we
25 simplified the theoretical framework and modified the partitioning protocol.

26 **Keywords:** quantum mechanics/molecular mechanics; molecular dynamics; Adaptive QM/MM;
27 condensed matter; solvation

28

29 **1. Introduction**

30 In molecular simulations, the choice of molecular models has been a major concern and always
31 a product of compromise between accuracy and computational cost. To optimize this balance,
32 multiscale simulations, which combine more than two molecular models, have been proposed by
33 many research groups. Among the various multiscale techniques, the quantum-mechanical
34 (QM)/molecular-mechanical (MM) method has been the most popular and successful one. While QM
35 methods are transferable and accurate because they explicitly treat the electronic structure, they
36 require massive computation time and resources. Therefore, they have severe limitations regarding
37 the size of the systems that can be treated and the simulation times that can be achieved. In the
38 contrast, the QM/MM method makes partial electronic structures of gigantic systems available with
39 moderate computational load. Thus, it has been widely applied to investigate reactions in
40 biomolecules and solutions. To apply QM/MM methods within a molecular dynamics (MD)
41 simulation framework, there are two possible options. The first one is to define only the solute
42 molecule as QM and the rest as MM. The second option is to expand the QM region to the
43 surrounding solvent molecules. Apparently and intuitively, the latter option seems to yield a more
44 reasonable and natural picture of the molecular structure and dynamics because of the incorporation

45 of environmental quantum chemical effects. Regarding dynamics simulations, however, mobile
46 solvent molecules diffuse away from the QM solute in course of time. As a result, the solvent
47 quantum effect is lost, although the computational cost remains substantially larger than in the
48 former setting, which treats all solvent molecules as MM. Therefore, in conventional QM/MM MD
49 simulations, quantum chemical solvent effects cannot be taken into consideration.

50 To overcome this limitation, various corrective approaches have been proposed by several
51 research groups in the last two decades [1-10]. These approaches are categorized into two groups:
52 “constrained” and “adaptive” QM/MM methods. The constrained methods, such as “flexible inner
53 region ensemble separator” (FIRES) [1], “boundary based on exchange symmetry theory” (BEST) [2],
54 and “boundary constraint with correction” (BCC) [3], employ constraints on QM (and MM) solvent
55 molecules to prevent their diffusion. These methods are relatively stable, in particular the
56 Hamiltonian is well conserved in BCC. In addition, their computational cost is moderate compared
57 to that of the methods belonging to the other group because a particular division of the molecular
58 system into QM and MM regions, which is termed a QM/MM partitioning, is fixed during the
59 simulation. Since the “constrained” methods do not allow the exchange of solvent molecules through
60 the QM/MM border, their dynamics is not realistic. Instead, they are designed to investigate solvation
61 structures (e.g., through the calculation of radial distribution functions) using ensemble averages.
62 These methods are controversial because they assume that ensemble averages are rigorously accurate
63 only if there is a symmetric exchange between QM and MM solvent molecules; i.e., they suppose that
64 QM and MM solvent molecules are energetically identical.

65 In contrast to the constrained methods, adaptive QM/MM methods employ a flexible molecular
66 definition and allow exchanges between QM and MM molecules. To this end, most adaptive QM/MM
67 methods exploit a multipartitioning approach, which considers various QM/MM partitionings whose
68 QM regions consist of different sets of solvent molecules. Based on the respective partitionings,
69 potential energies and forces are individually calculated, and then the effective energy and forces,
70 which are used to update the coordinates along the MD simulation, are obtained as a weighted
71 average. The adaptive QM/MM methods, such as ONIOM-XS [5], buffered-force [6], permuted
72 adaptive partitioning (PAP) [7], sorted adaptive partitioning (SAP) [7], difference-based adaptive
73 solvation (DAS) [8], scaled interaction single partition adaptive (SISPA) [9], and size-consistent
74 multipartitioning (SCMP) [10], vary in the definition of the partitioning scheme and weight function.
75 For comparison, most constrained and adaptive methods are also termed “single-partitioning” and
76 “multipartitioning” methods, respectively. Since the computational cost to calculate energy and
77 forces depends on the number of QM/MM partitionings, adaptive QM/MM methods require
78 substantial computational resources except in the case of SISPA, which is based on a single-
79 partitioning approach.

80 In the adaptive QM/MM methods, the stability of the simulations is a major concern. To have
81 stable simulations, an adequate choice of weight function is key, and the conservation of the
82 Hamiltonian is an important index. Because of solvent diffusion, in adaptive methods, partitionings
83 have to be redefined to keep the solute of interest surrounded by QM solvent molecules, although
84 the abrupt update of partitionings can cause a discontinuity in the potential energy surface. Thus, a
85 weight function is introduced to silence contributions from updated partitionings. However, in most
86 adaptive methods, the weight function cannot completely remove the aforementioned discontinuity.
87 On the contrary, the weight function sometimes causes additional discontinuities. In many cases,
88 defective weight functions result in drastic temperature drifts under microcanonical (*NVE*)
89 conditions, as reviewed by Buló et al. [11]. To keep a constant temperature and stabilize the MD
90 simulations, a system may be linked to a thermostat (*NVT* ensemble). However, averaged observables
91 are not physically accurate if the Hamiltonian is not conserved. We proposed the size-consistent
92 multipartitioning (SCMP) QM/MM method in 2014 [10], which numerically conserve Hamiltonian
93 and lead to stable MD simulations over hundreds of pico second.

94 Because the force and energy calculations for each partitioning are independent in multipartitioning
95 methods, adaptive QM/MM methods can be trivially parallelized. However, most of them are based
96 on multiscale multipartitioning, in which the size of the QM regions varies among partitionings.

97 Therefore, the computational loads due to the energy and force calculations are inhomogeneous
98 among the respective partitioning, which causes idle time at several computational nodes. In contrast,
99 all partitionings in the SCMP method have the same number of QM solvent molecules; thus, the
100 SCMP method has high affinity with parallel computing.

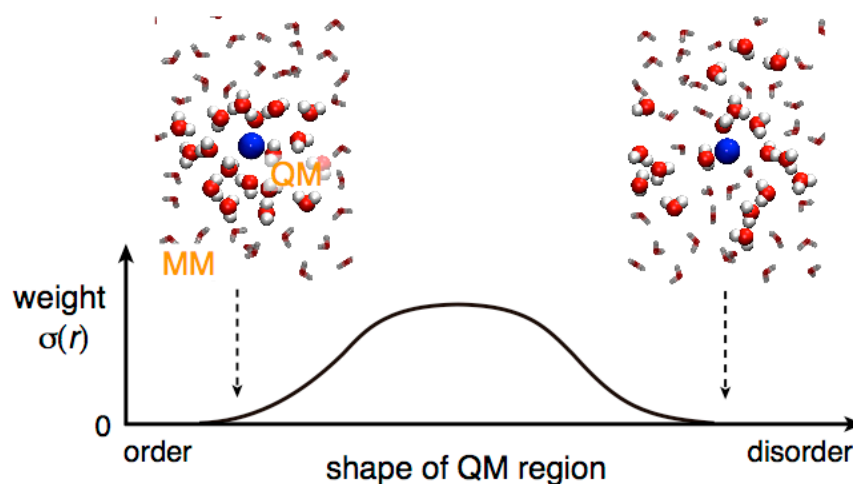
101 As practical applications, we have employed the SCMP methods to evaluate physicochemical
102 properties of water and monoatomic cation solutions [12,13]. Then, we demonstrated that quantum
103 chemical solvent effects exert a great impact on the solvation structure and dynamics of these systems
104 by evaluating their radial distribution function, infrared spectrum, and diffusion coefficient.

105 Although the SCMP method has shown high performance and potential, it still has vulnerability
106 because of the weight functions, where all the weights can be zero for certain situations, and, as a
107 result, MD simulations can crash. Furthermore, in previous studies, we also confirmed that the SCMP
108 can connect the QM and MM regions continuously on time average, but the spatial continuity is not
109 necessarily ensured at every MD time step. Moreover, the importance of the instantaneous spatial
110 continuity has not been discussed yet. Additionally, although the SCMP method theoretically should
111 keep its MD performance even for highly parallelized computing, the potential was not fully elicited
112 in a previous study [13]. Thus, in the present study, we propose modification of the SCMP theoretical
113 framework to increase MD performance, simulation stability, and spatial continuity. Then, we carry
114 out benchmark simulations for pure water and demonstrate the updated performance.
115

116 2. Theory

117 2.1. Size-consistent partitioning

118 Let us consider a solution system that consists of a solute of interest and M solvent molecules.
119 Then, suppose a QM/MM partitioning where the QM region consists of a solute and m solvent
120 molecules. Likewise, different QM/MM partitionings can be defined so that they share the same
121 solute molecule as QM and have consistently m solvent molecules in the QM region, but with
122 different sets of solvent molecules. The number of the possible QM/MM partitionings is $C_{(M,m)}$, and
123 thus, it is not feasible to computationally cover all of them. To reduce the number of partitionings to
124 be considered, we introduce a weight function σ that satisfies the following boundary conditions: σ
125 = 0 in the limit of ordered and disordered partitionings as shown in Scheme 1. Here, we define a
126 partitioning as ordered if all the nearest m solvent molecules to the QM solute are QM. Since the QM
127 solvent molecules diffuse away from the solute in a QM/MM partitioning, the QM region is supposed
128 to be disordered in the course of the MD simulation.



129 **Scheme 1.** Concept of weight function. The horizontal axis represents a conceptual index related to
130 the degree of disorder of the QM region.

131 If a partitioning has a perfectly ordered QM region at a given MD simulation time step, it should
132 have a weight of zero and no contribution to the dynamics. Because of the solvent diffusion, the

133 weight of the partitioning becomes greater than zero as the simulation evolves, and then, the weight
 134 gradually goes back to zero again when the QM region is completely disordered. Because of the
 135 aforementioned conditions, a substantial number of partitionings have a weight of zero and are
 136 screened out. Although countless partitionings can still have nonzero weight, the size-consistent
 137 partitioning allows to take into account only a finite number N of partitionings to obtain the effective
 138 energy and force on each atom.

139 The SCMP method is supposed to be parallelized via Message Passing Interface (MPI), where
 140 the energy and force calculations of each QM/MM partitioning are assigned to a single node. Thus, a
 141 QM/MM partitioning having a completely disordered QM region is replaced by another one having
 142 a completely ordered QM region at the same time step. Since both completely ordered and disordered
 143 partitionings are zero-weighted, the partitioning updates do not cause any discontinuity in the
 144 effective energy and forces along the MD simulation.

145 146 2.2. Score Function

147 To numerically describe the condition $\sigma^{(n)}$ mentioned in Section 2.1, we define a score function
 148 for a solvent molecule j in the n -th partitioning as $\Lambda_j^{(n)}$. According to the molecular definition, this
 149 score function varies as follows:

$$\Lambda_j^{(n)} = \begin{cases} \lambda_{j,\text{QM}}^{(n)}(r_j) & \text{if } j \in S_{\text{QM}}^{(n)} \\ \lambda_{j,\text{MM}}^{(n)}(r_j) & \text{if } j \notin S_{\text{QM}}^{(n)} \end{cases} \quad (1)$$

150 where a subgroup $S_{\text{QM}}^{(n)}$ contains the QM solvent molecules in the n -th partitioning, and r_j is the
 151 distance between the QM solute and the nearest j -th solvent molecule; $\lambda_{\text{QM}}(r_j)$ is a score function for
 152 a QM solvent, which are parameterized by range parameters s_{QM} , and t_{QM} ($\lambda_{\text{QM}}(r_j) = 1$ if $r_j \leq s_{\text{QM}}$, and
 153 $\lambda_{\text{QM}}(r_j) = 0$ if $t_{\text{QM}} \leq r_j$). Likewise, $\lambda_{\text{MM}}(r_j)$ is a score function for an MM atom using s_{MM} , and t_{MM} ($\lambda_{\text{MM}}(r_j)$
 154 $= 0$ for $r_j \leq s_{\text{MM}}$, and $\lambda_{\text{MM}}(r_j) = 1$ for $t_{\text{MM}} \leq r_j$). In the present study, we employed spline curves for λ_{QM}
 155 so that

$$\lambda_{\text{QM}}(s) = 1, \quad \lambda_{\text{QM}}(t) = 0, \quad \left. \frac{\partial \lambda_{\text{QM}}}{\partial r} \right|_{s,t=0} = 0, \quad \left. \frac{\partial^2 \lambda_{\text{QM}}}{\partial r^2} \right|_{s,t=0} = 0. \quad (2)$$

156 Also, λ_{MM} satisfies

$$\lambda_{\text{MM}}(s) = 0, \quad \lambda_{\text{MM}}(t) = 1, \quad \left. \frac{\partial \lambda_{\text{MM}}}{\partial r} \right|_{s,t=0} = 0, \quad \left. \frac{\partial^2 \lambda_{\text{MM}}}{\partial r^2} \right|_{s,t=0} = 0. \quad (3)$$

157 158 2.3. Fade-in and Fade-out Functions

159 Using the score function introduced in Section 2.2, the fade-out function $O_{\text{QM}}^{(n)}$ is defined for the QM
 160 solvent molecules in the n -th partitioning as follows:

$$O_{\text{QM}}^{(n)} = \prod_{j \in S_{\text{QM}}^{(n)}} \Lambda_j^{(n)}(r_j) \quad (4)$$

161 Note that $O_{\text{QM}}^{(n)} = 0$ if any QM solvent molecules in the n -th partitioning diffuses far away (beyond
 162 s_{QM}) from the QM solute. Otherwise, $O_{\text{QM}}^{(n)} > 0$. Next, we define the fade-in function $I^{(n)}$ for the QM
 163 solvent molecules in the n -th partitioning as follows:

$$I_{\text{QM}}^{(n)} = 1 - \prod_{j \in S_{\text{QM}}^{(n)}} \Lambda_j^{(n)}(r_j) \quad (5)$$

164 $I_{\text{QM}}^{(n)} = 0$ if all the QM solvent molecules in the n -th partitioning are within s_{QM} from the QM solute.
 165 Otherwise, $I_{\text{QM}}^{(n)} > 0$.

166 Likewise, we also introduce the fade-out function $O_{\text{MM}}^{(n)}$ and the fade-in function $I_{\text{MM}}^{(n)}$ for the MM
 167 solvent molecules in the n -th partitioning, respectively

$$O_{\text{MM}}^{(n)} = \prod_{j \notin S_{\text{QM}}^{(n)}} \Lambda_j^{(n)}(r_j) \quad (6)$$

168

$$I_{\text{MM}}^{(n)} = 1 - \prod_{j \in S_{\text{QM}}^{(n)}} \Lambda_j^{(n)}(r_j) \quad (7)$$

169 In contrast to the functions defined for the QM part, $O_{\text{MM}}^{(n)} = 0$ if any MM solvent molecules in the n -
 170 th partitioning come within s_{MM} of the QM solute. Otherwise, $O_{\text{MM}}^{(n)} > 0$. On the other hand, $I_{\text{MM}}^{(n)} = 0$
 171 if all the MM solvent molecules in the n -th partitioning are far away (beyond t_{MM}) from the QM solute.
 172 Otherwise, $I_{\text{MM}}^{(n)} > 0$.

173

174 2.4. Weight Functions, Effective Energy, and Forces

175 Using the fade-in and fade-out functions, the SCMP weight function of the n -th partitioning, $\sigma^{(n)}$, can
 176 be written as:

$$\sigma^{(n)} = \frac{O_{\text{QM}}^{(n)} I_{\text{QM}}^{(n)} O_{\text{MM}}^{(n)} I_{\text{MM}}^{(n)}}{\sum_k O_{\text{QM}}^{(k)} I_{\text{QM}}^{(k)} O_{\text{MM}}^{(k)} I_{\text{MM}}^{(k)}} \quad (8)$$

177 Note that $\sigma^{(n)}$ satisfies the previously mentioned boundary conditions. Then, the effective potential
 178 energy V^{eff} in MD simulations is

$$V^{\text{eff}}(\mathbf{r}) = \sum_n^N \sigma^{(n)}(\mathbf{r}) V^{(n)}(\mathbf{r}) \quad (9)$$

179 Since the weight function σ is normalized, the resulting effective forces and energy are always kept
 180 in a physically plausible scale, even if limited number of partitionings are considered, which is one
 181 of the advantages of using a size-consistent multipartitioning scheme. Furthermore, because the
 182 weight functions are perfectly continuous, the partitioning update does not cause any abrupt changes
 183 in the effective energy and forces.

184

185 3. Modification of the Update Protocol

186 The MD stability problem arises from the character of the SCMP weight function; the weight
 187 functions can become zero in limit of ordered or disordered partitioning. In addition, the number of
 188 partitionings to be considered is limited in practice. As a result, it is possible to have only a small
 189 number of partitionings with large weights, which would cause problems of stability and spatial
 190 continuity.

191 To better understand the stability problem, consider a solvent molecule that is defined as QM in
 192 all the weighted partitionings. If the QM solvent molecules diffuse beyond t_{QM} from a QM solute
 193 molecule, all the partitionings can have simultaneously a weight of zero, which would result in the
 194 collapse of the MD simulation. This would also be the case for the solvent molecules that are defined
 195 as MM in all the weighted partitionings. Therefore, to achieve the stability of the MD simulations, the
 196 partitionings should have variety in the selection of the QM solvent molecules and as many
 197 partitionings as possible should have nonzero weight. To assess simulation stability, let us define σ_{max}
 198 as

$$\sigma_{\text{max}} = \max(\sigma^{(1)}, \sigma^{(2)}, \dots, \sigma^{(n)}) \quad (10)$$

199 Note that σ_{max} ranges from $1/N$ to 1, where N represents the total number of partitionings. To achieve
 200 stable simulations, σ_{max} should be kept as small as possible.

201 Spatial continuity denotes a smooth connection between QM and MM regions. In other words,
 202 solvent models are smoothly alternated when solvent molecules cross the QM/MM border. To

203 intuitively understand spatial continuity, in a previous study [10], we introduced a useful measure:
 204 the QM profile $w_t(j)$

$$\omega_t(j) = \sum_n^N \sigma_t^{(n)} \delta(j) \quad (11)$$

205 which describes how much a solvent molecule that is the j -th nearest neighbor to the QM solute
 206 behaves as a QM molecule [10].

207 A QM profile is evaluated for each solvent molecule and ranges from 0 to 1 where the values of
 208 unity or zero indicate that the solvent molecule corresponds to a perfectly QM or MM model,
 209 respectively. Thus, as a solvent molecule approaches to the QM solute, the QM profile should become
 210 larger, and vice versa. Therefore, to have a smooth connection between the QM and MM regions, the
 211 QM profiles should gradually and monotonically decrease as the molecular number j increases.

212 213 3.1. Partitioning Update Types

214 In this section, we discuss the SCMP update types and modify the previous update scheme for
 215 efficiency. Let a QM inside entry be a process where a partitioning with $\sigma = 0$, because of either $I_{QM} =$
 216 0 or $I_{MM} = 0$, at a certain MD step becomes effectively weighted at the next MD step. Likewise, let MM
 217 inside entry be a process where a partitioning has nonzero weight because $I_{MM} > 0$. Here, we note that
 218 inside updates are not always available depending on the range parameters s and t . For example,
 219 suppose all partitionings have consistently m QM solvent molecules. Let d_j be the distance between
 220 the QM solute and the j -th nearest solvent molecule. Note that $I_{QM} = 0$ for $s_{QM} \geq d_m$, and $I_{MM} = 0$ for d_{m+1}
 221 $\geq t_{MM}$. Since d_j fluctuates during the MD simulations, if $t_{MM} > s_{QM}$, there can be a moment in which t_{MM}
 222 $> d_{m+1} \geq d_m > s_{QM}$. In this case, partitionings satisfying either $I_{QM} = 0$ or $I_{MM} = 0$ do not exist. If $s_{QM} \geq t_{MM}$,
 223 In contrast, there always exists at least one zero-weighted partitioning satisfying either $I_{QM} = 0$ or I_{MM}
 224 $= 0$ regardless of d_m . To make the update available at every MD time step, we assume $s_{QM} \geq t_{MM}$
 225 hereafter.

226 Next, let us compare the conditions $s_{QM} = t_{MM}$ and $s_{QM} > t_{MM}$. To have stable simulations, ideally,
 227 partitionings should have nonzero weights immediately after the update. Suppose that an updated
 228 partitioning with $\sigma = 0$ has $I_{QM} = 0$ for $s_{QM} > d_m$. Because of the diffusion of the QM solvent molecules,
 229 sooner or later, the updated partitioning by inside entry will have a nonzero weight, when $s_{QM} < d_m$.
 230 However, if $s_{QM} \gg d_m$, it would take time for the partitioning to have a nonzero weight; as a result, a
 231 small number of partitionings would have large weights, making the simulation unstable. Thus, s_{QM}
 232 should be as small as possible. For the same reason, t_{MM} should be as large as possible. Therefore, we
 233 assume that $s_{QM} = t_{MM}$ is the most efficient situation to suppress σ_{max} , and this will be the condition
 234 that we will apply for efficient update unless otherwise stated.

235 Let a QM outside entry be a process where a disordered partitioning with $\sigma = 0$ because $O_{QM} = 0$
 236 happens to be reweighted again. For instance, suppose that a QM solvent molecule diffuses beyond
 237 t_{QM} and accordingly $O_{QM} = 0$. Then, the diffused QM solvent molecule may happen to come back
 238 within t_{QM} again, leading to $\sigma > 0$ with $O_{QM} > 0$. Likewise, let an MM outside entry be a process where
 239 $\sigma > 0$ when an MM solvent molecule moves beyond s_{MM} of the QM solute. In contrast to the QM
 240 entries, the MM entries are always available regardless of range parameters s and t .

241 Note that partitionings updated by any of the four types, in particular MM inside and QM
 242 outside entries, may not necessarily be weighted again. For instance, while waiting for $\sigma > 0$ by a QM
 243 outside entry, the MM fade-out functions can become $O_{MM} = 0$. In such case, it is less likely that this
 244 partitioning can have a nonzero weight again in the limited simulation time. Thus, partitionings
 245 updated should be carefully checked to see if there are better candidates with nonzero weights among
 246 other possible partitionings. In contrast, a QM outside entry seems to happen more frequently
 247 because the sphere surface at $r = t_{QM}$ is larger than those at $r = s_{MM}$ and s_{QM} , and therefore, the frequency
 248 of solvent molecules crossing the surface is also higher.

249 We also note that, in previous studies, we made only use of the inside entry for partitioning
 250 update. In this case, limited partitionings are available for update, which seems to be inefficient, if
 251 many partitionings have to be updated at the same time because of partitioning overlap. In the

252 present study, we propose to exploit the outside entries to effectively control σ_{\max} . For efficiency,
253 when a partitioning becomes disordered ($\sigma=0$ by either $O_{\text{QM}}=0$ or $O_{\text{MM}}=0$), we make the partitioning
254 partially-ordered by tuning the solvent molecules irrelevant to $O=0$. Otherwise, as previously
255 mentioned, the outside-entered partitioning is highly likely to become disordered again.

256 257 3.2 Degree of Order

258 Under the condition that the range parameters $s_{\text{QM}} = t_{\text{MM}}$, the perfectly ordered partitioning
259 whose QM region consists of the nearest m solvent molecules has always zero weight as described in
260 the previous section. Using this property, in a previous study, we employed a minimum update
261 protocol where the partitioning to be updated is always replaced by the perfectly ordered
262 partitioning, namely the QM region consists of the nearest solvent molecules. Note that when the
263 minimum update is once performed, the partitioning update is not available until solvent diffusion
264 occurs to some extent. Otherwise, more than one partitioning can become identical. As a result, idling
265 times can happen between partitioning updates, which can cause an increase of the maximum weight
266 σ_{\max} and destabilize the MD simulation. Thus, the minimum update protocol is inefficient.

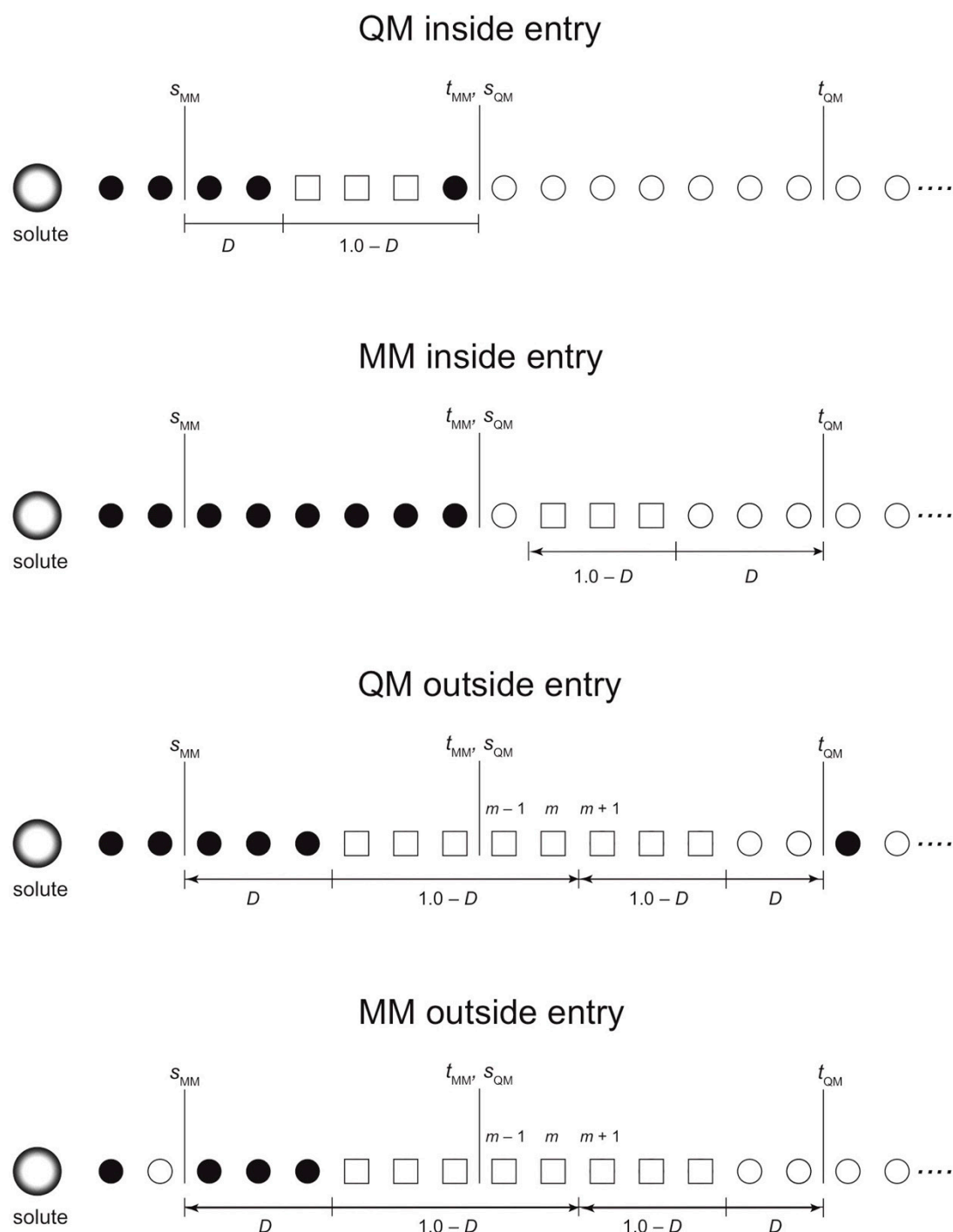
267 Here, we make the partitioning update more flexible by introducing an index, degree of order
268 (D). Note that either $I_{\text{QM}}O_{\text{QM}}$ or $I_{\text{MM}}O_{\text{MM}}$ is zero in a new partitioning, while the nonzero one is arbitrary.
269 Thus, keeping $\sigma=0$, new partitionings can be disordered to some extent. The degree of order D
270 indicates how ordered a new partitioning is. If $D=1$, the fade-in function $I=0$ ($O=1$), and the scenario
271 is equivalent to that of the minimum update. If $D=0$, $I=1$ ($O=0$), which indicates that the partitioning
272 is already completely disordered. The four types of update protocols in combination with the degree
273 of order are visualized in Scheme 2 and detailed in Appendix A. We assume that the optimal value
274 of D makes the updated partitionings to become effectively weighted after an entry. Although the
275 optimal value of D is not trivial, it should obviously be between $D=0$ and $D=1$. Thus, we assessed
276 the optimal value of D in the section below.

278 4. Results

279 4.1. MD Performance

280 Figure 1 indicates the relative MD performances against the conventional QM/MM simulations.
281 In MD simulations, in particular for QM/MM systems, the computational loads are mainly attributed
282 to the force and energy calculations. The SCMP simulation is designed carried out in parallel, and the
283 force and energy calculations for the individual partitionings are assigned to the respective
284 computational nodes. Thus, in parallel computing, the SCMP simulations should theoretically keep
285 high MD performance, namely wall-time per MD step, even when the number of partitionings
286 increases. Nevertheless, in previous studies, MD performance was substantially affected by the
287 number of partitionings [13], which implies that computational loads specific to the SCMP method,
288 namely the weight calculations, are comparable to the force and energy calculations. This agrees with
289 the fact that the linear extrapolation of the SCMP performance does not agree with that of the
290 conventional QM/MM MD simulations, based on a single partitioning. We find that most parts of the
291 weight calculations, that imply the evaluations of the score and fade-in/out functions, are fortunately
292 independent among partitionings, and thus they can be also trivially parallelized.

293 Furthermore, the fade-out and fade-in functions share the same score functions \mathcal{A} as in Eq (4-7).
294 Although it is necessarily required to share the functions, there is no legitimate reason to use different
295 functions. Since the sharing eliminates redundancy, it is advantageous with respect to the
296 computational cost; in addition, the SCMP overview and programming is simplified. Thus, in the
297 following section, we use the same range parameters s and t for the QM and MM score functions.



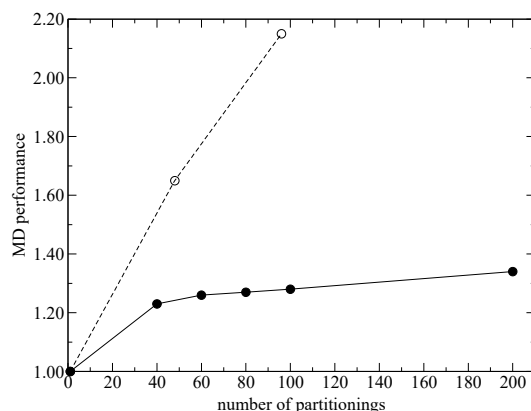
298
299

Scheme 2. Four possible patterns of partitioning update. Filled and open circles represent QM and MM solvent, respectively. The open squares stand for either QM or MM solvent.

300
301
302
303
304
305
306
307

To assess MD performance in the weight calculations via parallelization and parameter sharing, we conducted benchmark simulations on a computer server with an Intel Xeon E5-2670v2 CPU. As shown in Figure 1, the present study successfully elicited the potential efficiency of the SMCP method and showed high MD performance and robustness with respect to the number of partitionings. Note that the MD performance shows slightly linear dependency on the number of partitionings, which seems to be originated from the partitioning update in the SCMP simulation. Thus, room may still remain for further improvement, although its parallelization is not as straightforward as that of the weight calculation.

308



309 **Figure 1.** MD performances (wall-time per one MD step) of the SCMP simulations relative to a
310 conventional QM/MM simulation that has the same size of the QM region. Filled circles and the solid
311 line represent the results in the present study, and open circles and the dashed line represent the
312 results in a previous study [13]. The benchmark simulations were conducted for a system composed
313 by 2048 water molecules, where the QM region consisted of one solute water and 32 solvent water
314 molecules.

315

316

317

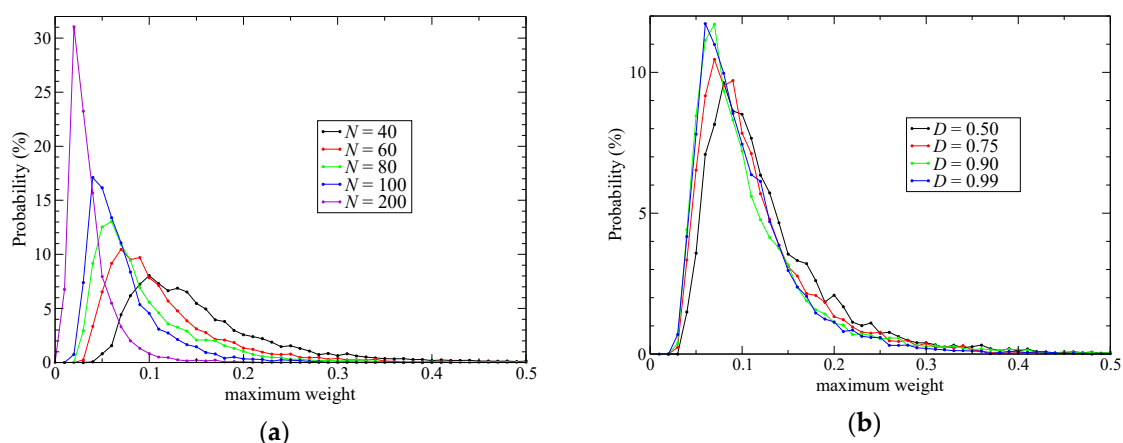
4.2. Simulation Stability

318 To evaluate simulations stability, we conducted SCMP simulations with different numbers of
319 partitionings (40, 60, 80, 100, and 200) and evaluated the distribution of σ_{\max} sampled along the MD
320 simulations as shown in Figure 2a. As expected, the maximum value of the partitioning weights
321 obviously depends on the number of partitionings; a larger number of partitionings leads to a smaller
322 σ_{\max} value.

323 Next, we evaluated the distribution of σ_{\max} for a SCMP simulation with 60 partitionings using
324 various degrees of order ($D = 0.50, 0.75, 0.90,$ and 0.99) as shown in Figure 2b. Notably, a larger value
325 of D seems to keep σ_{\max} smaller, although there is not a distinct difference for $D = 0.90$ and 0.99 . Thus,
326 we conclude that in what regards simulation stability, the optimal value of D seems to be between
327 0.90 and 0.99 . On the contrary, we emphasize that all the simulations conducted in the present study
328 lasted for 100 ps and never collapsed even with an unfavorable condition such as $D = 0.50$. This is in
329 contrast to previous studies where the MD simulations sometimes crashed. We think that
330 stabilization is achieved because of the new partitioning update protocol. While we used only two
331 protocols (QM and MM inside entries) in previous studies, we made use of four types of the
332 partitioning update protocol in the present study (see Appendix).

333

334



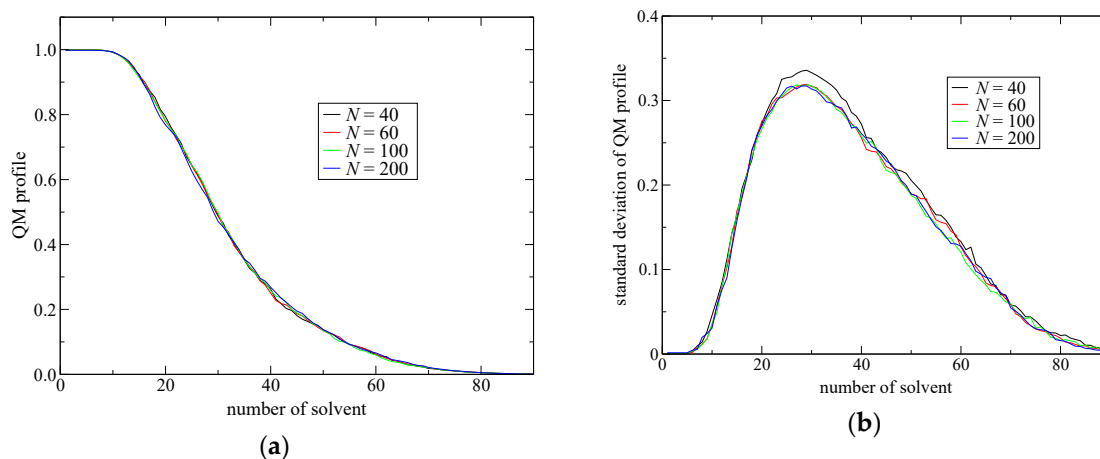
335 **Figure 2.** Distribution of the maximum value, $\sigma_{\max}(t)$, sampled over 100 ps MD simulations where
 336 respective partitionings contain 1 QM solute and 32 QM solvent molecules. (a) The black, red, green,
 337 blue, and purple lines represent the simulations with 40, 60, 80, 100, and 200 partitionings,
 338 respectively. All the simulations employed $D = 0.75$. (b) The black, red, green, and blue lines represent
 339 the results from the simulations with $D = 0.50, 0.75, 0.90,$ and 0.99 , respectively; all the simulations
 340 were performed with 60 partitionings.

341 4.3. Spatial Continuity

342 To assess the spatial continuity, we compared the QM profiles obtained from SCMP simulations
 343 employing different number partitionings (40, 80, 100, and 200). The QM profiles are subject to the
 344 score function in Eq (1), although it is not straightforward to guess the form of the QM profile from
 345 the score function. As shown in Figure 3a, the time-averaged QM profiles over the MD simulations
 346 smoothly and monotonically decrease as the distance from the QM center increases. In addition, they
 347 are not affected by the number of partitionings at least in the range from 40 to 200 partitionings.
 348 Therefore, spatial continuity seems to be achieved with respect to time average. However, this does
 349 not necessarily ensure instantaneous spatial continuity, which is defined at every MD time step.

350 To discuss instantaneous spatial continuity, we focused on the standard deviations (SDs) of the
 351 QM profiles. As shown in Figure 3b, SDs are remarkably large, with a maximum value of about 0.3
 352 at around the 32nd solvent molecule from the QM solute, which notably agrees with the number of
 353 QM solvent molecules in the respective partitionings. These large SDs imply that the QM profiles
 354 significantly fluctuate in the course of the MD time, and the instantaneous QM profiles may not
 355 necessarily decrease monotonically. As a result, the entire shape of the instantaneous QM profiles
 356 does not agree with the expected shape displayed in Figure 3a. We emphasize that, if all possible
 357 size-consistent partitionings are considered, perfect instantaneous spatial continuity should be
 358 achieved. Therefore, as the number of partitionings increases, the SDs of the QM profiles should be
 359 reduced. Notably, however, Figure 3b shows that the increase in the number of partitionings in the
 360 range from 60 to 200 does not cause the decrease of the associated SD, although the SDs
 361 corresponding to the QM profile obtained from the SCMP simulation carried out with 40
 362 partitionings is the largest.

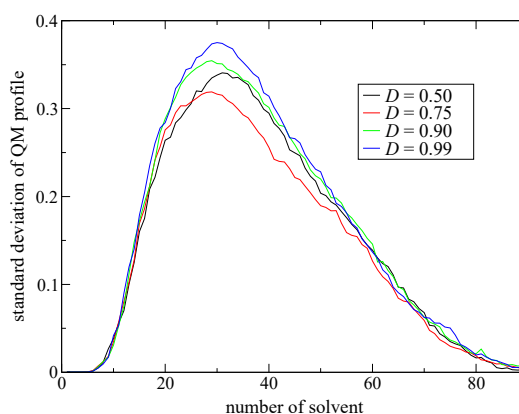
363



364 **Figure 3.** (a) Time-averaged QM profiles, and (b) their standard deviations obtained from 100 ps
 365 SCMP simulations. The horizontal axis represents the solvent number from the QM solute. Black, red,
 366 green, and blue lines represent the results obtained by the SCMP method with number of
 367 partitionings equal to 40, 60, 100, and 200, respectively.

368 Next, we assessed the SDs of the QM profiles obtained using 60 partitionings and different
 369 degrees of order $D = 0.50, 0.75, 0.90,$ and 0.99 . Figure 4 indicates that SDs vary depending on D ; $D =$
 370 0.75 gives the smallest SD value, namely the best spatial continuity. Notably, the values of D that lead
 371 to the best spatial continuity and the best simulations stability are not the same.

372
 373

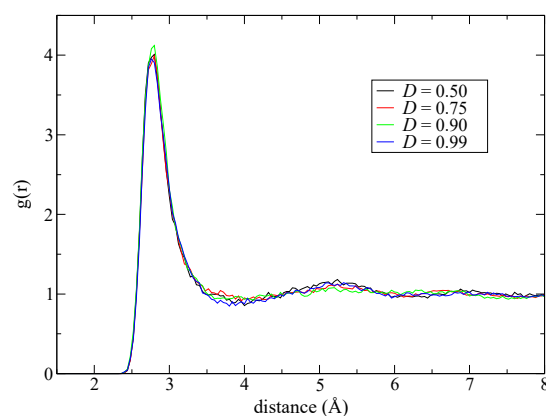


374 **Figure 4.** Standard deviations of instantaneous QM profiles obtained from 100 ps SCMP simulations
 375 with 60 partitionings containing one QM solute water and 32 QM solvent water molecules. The
 376 horizontal axes represent the solvent number from the QM solute. Black, red, green, and blue lines
 377 represent the results obtained by SCMP with degrees of order $D = 0.50, 0.75, 0.90,$ and $0.99,$
 378 respectively.

379 To evaluate the effect of spatial continuity on solvation structure, we calculated the time-
 380 averaged QM solute oxygen-centered radial distribution functions for the solvent oxygen atoms. As
 381 shown in Figure 5, notably, the radial distribution functions (RDFs) do not show any distinct
 382 difference for different values of D . We also did not observe any clear difference in the RDFs when
 383 compared to different number of partitionings (data not shown). Considering that all the present
 384 simulations realize smooth switching of the QM profiles on time-average (Figure 3a), and that the
 385 present RDFs are also time-averaged, it seems reasonable that the RDFs correspond to the time-
 386 averaged QM profiles (and not with the instantaneous QM profiles).

387 In a previous study, we showed that the dynamics of a single QM solute surrounded by MM
 388 solvent molecules, which is an extreme case of spatial discontinuity, is neither equivalent to that of a

389 pure QM system nor to that of an MM one. Thus, if the QM and MM regions are directly connected
390 as in most of the single-partitioning QM/MM methods, the solvent molecules around the QM/MM
391 border can show unphysical behaviors. In contrast, the gradual transition of solvent molecules
392 between QM and MM is not physically legitimate, but it is an implicitly required condition in
393 multipartitioning methods. Indeed, some multipartitioning methods such as PAP, SAP and DAS are
394 designed to perfectly achieve spatial continuity at every MD time step, and Park et al. demonstrated
395 by using the DAS method that the location of the transition region can affect the resulting physical
396 quantity [14], although this effect cannot be attributed only to spatial continuity problems because
397 SAP and DAS cannot deal with temporal discontinuity problems. Therefore, it still remains an open
398 question which connection can yield more reasonable results. Although we did not confirm any effect
399 of instantaneous spatial continuity in the present study, at least within the SCMP framework, it is
400 preferable to have a QM profile decreasing monotonically to suppress artifacts around the QM center
401 because of the QM/MM border.
402
403



404 **Figure 5.** RDFs obtained from 100 ps SCMP simulations with 60 partitionings. Black, red, green, and
405 blue lines represent the results obtained by SCMP with degrees of order $D = 0.50, 0.75, 0.90,$ and $0.99,$
406 respectively.

407

408 5. Computational Details

409 All the calculations were carried out with a local version of the GROMACS 5.0.7 package [15-18]
410 where we implemented the DFTB3 code provided by Dr. Tomáš Kubař [19] and our own SCMP code.
411 We employed DFTB3 [20] with 3OB parameters [21] to treat the molecules in the QM part and the
412 SPC-Fw model to describe MM water molecules. The electrostatic interactions within the MM part
413 were evaluated using the particle-mesh Ewald method [22] with a switching function from 8.5 to 9.0
414 Å. The MD simulations were conducted under periodic boundary conditions in the *NVE* ensemble,
415 with a time step of 0.5 fs, and after inserting 2048 H₂O molecules in a cubic box with a side length of
416 39.48 Å. The range parameters were set as $s_{MM} = 3.5$ Å and $t_{MM} = s_{QM} = 6.0$ Å, and $t_{QM} = 8.8$ Å.
417

418 6. Conclusions

419 The SCMP method enables to incorporate quantum chemical solvent effects in MD simulations.
420 First, in the present study, we proposed a simple form for the score functions used in the weight
421 evaluations and discussed an additional parallelization scheme. Then, we benchmarked the MD
422 performance and demonstrated that the SCMP potential efficiency was well elicited even for highly
423 parallel computations.

424 Next, to improve simulation stability and spatial continuity, we proposed new protocols for the
425 partitioning update and introduced an index, degree of order. We focused on the maximum weight
426 at every MD time step as a measure of the stability of the simulations. Then, we found an extended
427 partitioning update protocol that increases the simulation stability; as a result, we did not face any
428 collapse in the MD simulation performed in the present study. We also demonstrated that the number
429 of partitionings is directly connected to the simulation stability. In addition to the extended update
430 protocol, we introduced the degree of order, which affects simulation stability to some extent too.
431 Benchmark simulations showed that there is an optimal value for the degree of order, which
432 presumably depends on the simulation condition. For spatial continuity, we used the QM profile as
433 an index and demonstrated that the present simulations achieved spatial continuity on time average
434 over MD simulations regardless of the number of partitionings (at least in a range from 40 to 200).
435 Notably, however, instantaneous spatial continuity at every MD time step was not necessarily
436 satisfactory containing large errors. While the number of partitionings, which saturates around 60
437 partitionings, is not crucial to achieve instantaneous spatial continuity, the degree of order in the
438 partitioning update protocol seems to be influential. Concerning the degree of order, notably, the
439 optimal values to achieve spatial continuity and simulation stability do not necessarily match.
440 Because RDFs are also obtained by time-averaged analysis, we could not observe any distinct
441 difference in RDFs in what regards to instantaneous spatial continuity. There still remains room for
442 further research on evaluating spatial continuity.
443

444 **Author Contributions:** All the present research and paper writing was carried out by H.C.W.

445 **Funding:** This research was funded by JSPS KAKENHI Grant Number JP17K15101 and JST PRESTO Grant
446 Number JPMJPR17GC.

447 **Acknowledgments:** The computations were performed using the TSUBAME Encouragement Program for
448 Young/Female Users of Global Scientific Information and Computing Center at the Tokyo Institute of
449 Technology, and the Joint Usage/Research Center for Interdisciplinary Large-Scale Information Infrastructures
450 in Japan.

451 **Conflicts of Interest:** The author declares no conflict of interest. The founding sponsors had no role in the design
452 of the study; in the collection, analyses, or interpretation of data; in the writing of the manuscript; or in the
453 decision to publish the results.

454 Appendix

455 **QM inside entry:** Among the solvent molecules within s_{QM} of the QM solute, set the furthest solvent
456 QM. Let k solvent molecules be in the range from s_{MM} to $t_{MM}(s_{QM})$ from the QM center. The nearest D
457 $\times k$ solvent molecules are defined as QM, while the rest of k solvent molecules are defined as either
458 QM or MM molecules in a new partitioning.
459

460 **MM inside entry:** Among the solvent molecules more than t_{MM} from the QM solute, set the nearest
461 solvent MM, while the solvent within t_{MM} of the QM solute should be QM. Let k solvent molecules be
462 in the range from $t_{MM}(s_{QM})$ to t_{QM} from the QM center. The furthest $(1 - D) \times k$ solvent molecules are
463 defined as MM, while the rest of k solvent molecules are defined as either QM or MM molecules in a
464 new partitioning.
465

466 **QM outside entry:** Among the solvent molecules more than t_{QM} from the QM solute, the nearest one
467 should be QM. Suppose the QM region contains m QM solvent molecules, and the m -th solvent is at
468 a distance larger than r_m from the QM center. Let k solvent molecules ranging from r_m to t_{QM} from the
469 QM center. The furthest $D \times k$ solvents are defined as MM. The rest of the k solvents are defined as
470 either QM or MM. Likewise, let be l solvent molecules ranging from r_m to t_{QM} from the QM center.
471 The nearest $D \times l$ solvent molecules are defined as QM. The rest of the l solvent molecules are defined
472 as either QM or MM.
473

474 **MM outside entry:** Among the solvent molecules within S_{MM} of the QM solute, the furthest one
475 should be MM. Let the QM region contain m QM solvent molecules, and r_m be the distance between
476 the m -th solvent molecule and the QM center. Suppose k solvent molecules exist in the range from r_m
477 to t_{QM} . The furthest $D \times k$ solvent molecules are defined as MM. The rest of the k solvent molecules
478 are defined as either QM or MM. Likewise, let l solvent molecules exist in the range from r_m to t_{QM}
479 from the QM center. The nearest $D \times l$ solvent molecules are defined as QM. The rest of the l solvent
480 molecules are defined as either QM or MM.

481

482 **References**

483

- 484 1. Rowley, C.N.; Roux, B. The solvation structure of Na^+ and K^+ in liquid water determined from high level
485 ab initio molecular dynamics simulations. *J. Chem. Theory Comput.* **2012**, *8*, 3526–3535.
- 486 2. Shiga, M.; Masia, M. Boundary based on exchange symmetry theory for multilevel simulations. I. Basic
487 theory. *J. Chem. Phys.* **2013**, *139*, 044120.
- 488 3. Takahashi, H.; Kambe, H.; Morita, A. A simple and effective solution to the constrained QM/MM
489 simulations. *J. Chem. Phys.* **2018**, *148*, 134119.
- 490 4. Waller, M.P.; Kumbhar, S.; Yang, J. A density-based adaptive quantum mechanical/molecular mechanical
491 method. *Chemphyschem* **2014**, *15*, 3218–3225.
- 492 5. Kerdcharoen, T.; Morokuma, K. Oniom-xs: An extension of the ONIOM method for molecular simulation
493 in condensed phase. *Chem. Phys. Lett.* **2002**, *355*, 257–262.
- 494 6. Bernstein, N.; Varnai, C.; Solt, I.; Winfield, S.A.; Payne, M.C.; Simon, I.; Fuxreiter, M.; Csanyi, G. QM/MM
495 simulation of liquid water with an adaptive quantum region. *Phys. Chem. Chem. Phys.* **2012**, *14*, 646–656.
- 496 7. Heyden, A.; Lin, H.; Truhlar, D.G. Adaptive partitioning in combined quantum mechanical and molecular
497 mechanical calculations of potential energy functions for multiscale simulations. *J. Phys. Chem. B* **2007**, *111*,
498 2231–2241.
- 499 8. Buló, R.E.; Ensing, B.; Sikkema, J.; Visscher, L. Toward a practical method for adaptive QM/MM
500 simulations. *J. Chem. Theory Comput.* **2009**, *5*, 2212–2221.
- 501 9. Field, M.J. An algorithm for adaptive qc/mm simulations. *J. Chem. Theory Comput.* **2017**, *13*, 2342–2351.
- 502 10. Watanabe, H.C.; Kubar, T.; Elstner, M. Size-consistent multipartitioning qm/mm: A stable and efficient
503 adaptive qm/mm method. *J. Chem. Theory Comput.* **2014**, *10*, 4242–4252.
- 504 11. Buló, R.E.; Michel, C.; Fleurat-Lessard, P.; Sautet, P. Multiscale modeling of chemistry in water: Are we
505 there yet? *J. Chem. Theory Comput.* **2013**, *9*, 5567–5577.
- 506 12. Watanabe, H.C.; Banno, M.; Sakurai, M. An adaptive quantum mechanics/molecular mechanics method
507 for the infrared spectrum of water: Incorporation of the quantum effect between solute and solvent. *Phys.*
508 *Chem. Chem. Phys.* **2016**, *18*, 7318–7333.
- 509 13. Watanabe, H.C.; Kubillus, M.; Kubar, T.; Stach, R.; Mizaikoff, B.; Ishikita, H. Cation solvation with quantum
510 chemical effects modeled by a size-consistent multi-partitioning quantum mechanics/molecular mechanics
511 method. *Phys. Chem. Chem. Phys.* **2017**, *19*, 17985–17997.
- 512 14. Park, K.; Gotz, A.W.; Walker, R.C.; Paesani, F. Application of adaptive qm/mm methods to molecular
513 dynamics simulations of aqueous systems. *J. Chem. Theory Comput.* **2012**, *8*, 2868–2877.
- 514 15. Hess, B.; Kutzner, C.; van der Spoel, D.; Lindahl, E. Gromacs 4: Algorithms for highly efficient, load-
515 balanced, and scalable molecular simulation. *J. Chem. Theory Comput.* **2008**, *4*, 435–447.
- 516 16. Bjelkmar, P.; Larsson, P.; Cuendet, M.A.; Hess, B.; Lindahl, E. Implementation of the charmm force field in
517 gromacs: Analysis of protein stability effects from correction maps, virtual interaction sites, and water
518 models. *J. Chem. Theory Comput.* **2010**, *6*, 459–466.

- 519 17. Pronk, S.; Pall, S.; Schulz, R.; Larsson, P.; Bjelkmar, P.; Apostolov, R.; Shirts, M.R.; Smith, J.C.; Kasson, P.M.;
520 van der Spoel, D.; Hess, B.; Lindahl, E. Gromacs 4.5: A high-throughput and highly parallel open source
521 molecular simulation toolkit. *Bioinformatics* **2013**, *29*, 845–854.
- 522 18. Abraham, M.J.; Murtola, T.; Schulz, R.; Páll, S.; Smith, J.C.; Hess, B.; Lindahl, E. Gromacs: High performance
523 molecular simulations through multi-level parallelism from laptops to supercomputers. *SoftwareX* **2015**, *1*,
524 19–25.
- 525 19. Kubar, T.; Welke, K.; Groenhof, G. New qm/mm implementation of the dftb3 method in the gromacs
526 package. *J. Comput. Chem.* **2015**, *36*, 1978–1989.
- 527 20. Gaus, M.; Cui, Q.A.; Elstner, M. Dftb3: Extension of the self-consistent-charge density-functional tight-
528 binding method (scc-dftb). *J. Chem. Theory Comput.* **2011**, *7*, 931–948.
- 529 21. Gaus, M.; Goez, A.; Elstner, M. Parametrization and benchmark of dftb3 for organic molecules. *J. Chem.*
530 *Theory Comput.* **2013**, *9*, 338–354.
- 531 22. Darden, T.; York, D.; Pedersen, L. Particle mesh ewald - an n.Log(n) method for ewald sums in large
532 systems. *J. Chem. Phys.* **1993**, *98*, 10089–10092.